Pseudomonas syringae pv. *tomato* DC3000 induces defense responses in diverse maize inbred lines

Namrata Jaiswal[1] and Matthew Helm[1] *

[1] Crop Production and Pest Control Research Unit, U.S. Department of Agriculture-Agricultural Research Service (USDA-ARS), West Lafayette, IN 47907, U.S.A.

* **Corresponding author:** M. Helm; Email: Matthew.Helm@usda.gov

Funding

This research was funded by the United States Department of Agriculture, Agricultural Research Service (USDA-ARS) research project 5020-21220-014-00D. The funding bodies had no role in designing the experiments, collecting the data, or writing the manuscript. All opinions expressed in this paper are the author's and do not necessarily reflect the policies and views of USDA. USDA is an equal opportunity provider and employer.

ABSTRACT

Many phytopathogens translocate virulence (effector) proteins into plant cells to circumvent host immune responses during infection. One such pathogen is *Pseudomonas syringae* pv. *tomato* DC3000, which secretes at least twenty-nine effectors into host cells, of which a subset elicits host defense responses in crop plant species. However, it is unknown whether *P. syringae* pv. *tomato* DC3000 activates immune responses in diverse maize inbreds. Here, we screened a diverse maize germplasm collection for effector-dependent recognition of this bacterial pathogen. As a control, we infiltrated *Pseudomonas syringae* DC3000(D36E), a derivative of *P. syringae* pv. *tomato* DC3000 that lacks all endogenous effectors. In our evaluations, we observed a variety of responses to *P. syringae* pv. *tomato* DC3000 in maize and scored the phenotypes as either no observable response (N) or as one of three responses: weak chlorosis (WC), chlorosis (C) with minimal cell death, and hypersensitive reaction (HR)-like cell death. Of the twenty-six maize inbreds screened, 13 were scored as N, 2 as WC, 2 as C, and 9 as HR-like cell death. Importantly, no maize line responded to *P. syringae* DC3000(D36E), demonstrating the responses observed are likely dependent upon recognition of one or more *Pseudomonas* effectors. Importantly, maize inbreds that recognize *P. syringae* pv. *tomato* DC3000 accumulated detectable hydrogen peroxide as well as an increase in transcript expression of a subset of maize defense genes. Collectively, our results will likely stimulate new research aimed at identifying the cognate maize disease resistance proteins that recognize the activities of one or more bacterial effectors.

Key words: maize, *Pseudomonas syringae*, effector delivery, defense responses, ROS

INTRODUCTION

To facilitate disease development, plant phytopathogens often secrete a repertoire of virulence proteins, known as effectors, to host cells during the infection process (Bentham et al., 2020). The primary function of these pathogen-secreted effectors is to manipulate host cell physiology and development, including the structure and function of plant cells as well as modulate host immune responses (Bentham et al., 2020; Lovelace et al., 2023). To circumvent the immune-suppressing activities of diverse plant phytopathogens, plants have evolved a two-tiered, integrated immune signaling network (Bentham et al., 2020; Lovelace et al., 2023; Ngou et al., 2022). The first tier, often referred to as cell surface-triggered immunity, primarily involves the detection of pathogen-associated molecular pattern (PAMPs) by cell surface-localized, transmembrane immune receptors) (Bentham et al., 2020; Ngou et al., 2022). Upon recognition of pathogen-derived PAMPs, the host cell will initiate several coordinated defense responses including, in part, an increase in the production reactive oxygen species (ROS), stomatal closure, calcium influx and accumulation within the host cytosol, as well as up-regulation of defense-related genes (Bentham et al., 2020; Chen et al., 2022; Ngou et al., 2022). The second tier of the plant immune system is often mediated by intracellular innate immune receptors known as nucleotide-binding, leucine-rich repeat (NLR) proteins, whose primary function is to detect the activities of pathogen-secreted effectors inside host cells. Once activated, plant NLR proteins

70 initiate a cell death response, known as the hypersensitive reaction (HR), which is
71 thought to restrict pathogen growth and systemic spread (Bentham et al., 2020; Coll et
72 al., 2011; Ngou et al., 2022). This tier of host immunity is often referred to as effector-
73 triggered immunity (ETI) or intracellular receptor-mediated immunity (Ngou et al., 2022).
74 The bacterial phytopathogen *Pseudomonas syringae* pv. *tomato* DC3000 has
75 been foundational to the study of effector biology and its study has yielded significant
76 insights into the structure of the plant immune system (Wei and Collmer, 2018; Xin and
77 He, 2013). During pathogenesis, this hemibiotrophic pathogen colonizes the host
78 apoplast by entering through stomata and uses the type III secretion system (T3SS) to
79 deliver at least twenty-nine effector proteins directly into the host cell cytoplasm (Wei et
80 al., 2018; Xin and He, 2013). Once translocated, these effector proteins predominantly
81 function to suppress host immune responses or modulate host development, thereby
82 facilitating disease progression (Wei et al., 2018; Xin and He, 2013). For example, the
83 *P. syringae* pv. *tomato* DC3000 effector HopM1 suppresses both PAMP-elicited ROS
84 production as well as stomatal closure in Arabidopsis, thus facilitating disease
85 development (Lozano-Duran et al., 2014). Additionally, the HopK1 effector from *P.*
86 *syringae* pv. *tomato* DC3000 suppresses HR-like cell death elicited by another *P.*
87 *syringae* pv. *tomato* DC3000 effector, HopA1, as well as PTI responses including ROS
88 production and callose deposition (Guo et al., 2009; Jamir et al., 2004; Li et al., 2014).
89 Interestingly, HopK1 encodes a chloroplast transit peptide and accumulates in host
90 chloroplasts, suggesting chloroplast localization may be important for HopK1-mediated
91 suppression of PTI and ETI responses (Li et al., 2014). HopQ1 (also known as HopQ1-
92 1) is conserved across pathogenic bacteria and, intriguingly, induces an HR-like cell

93 death response when transiently expressed in *N. benthamiana* (Ferrante et al., 2009;
94 Wei et al., 2007). Upon *P. syringae* pv. *tomato* DC3000-dependent delivery into
95 Arabidopsis, AvrPto and AvrPtoB function redundantly to attenuate flagellin22 (flg22)
96 perception by the cell surface-localized immune receptor, FLS2 (Boller and Felix, 2009;
97 Kvitko et al., 2009; Martin, 2012).

98 The maize Nested Association Mapping (NAM) recombinant inbred lines (RILs)
99 representing global maize diversity were derived from twenty-six inbred founder lines
100 and are a valuable genetic resource for discovering allelic diversity against plant
101 pathogens of maize (Gage et al., 2020; Singh et al., 2023). For example, Kump and
102 colleagues (2011) used the NAM population to identify thirty-two quantitative trait loci
103 associated with resistance to *Cochliobolus heterostrophus*, the causative pathogen of
104 Southern Leaf Blight disease, in maize. Furthermore, this mapping population was also
105 used to identify the genetic resistance architecture underlying quantitative disease
106 resistance to Gray Leaf Spot (GLS) disease and Northern leaf blight (NLB) disease
107 (Benson et al., 2015; Poland et al., 2011). These studies thus demonstrate the value
108 and versatility of screening the NAM population for identifying maize disease resistance
109 genes. To the best of our knowledge, the maize NAM population has not been used to
110 identify putative sources of genetic resistance to *P. syringae* pv. *tomato* DC3000.

111 In the current study, we screened the maize NAM population for recognition of
112 the bacterial pathogen *P. syringae* pv. *tomato* DC3000. Of the twenty-six maize inbreds
113 evaluated in our screen, 13 were scored as having no observable response to *P.*
114 *syringae* pv. *tomato* DC3000. Two inbred lines were phenotyped as having a weak
115 chlorotic response and two as having a chlorotic response with minimal cell death. The

116 nine remaining maize inbreds all responded to *P. syringae* pv. *tomato* DC3000 with HR-
117 like cell death. Consistent with the phenotypic responses, the maize inbred lines that
118 recognized *P. syringae* pv. *tomato* DC3000 accumulated detectable hydrogen peroxide
119 within the infiltrated regions as well as an increase in transcript expression of a subset
120 of maize defense genes. As a control, we infiltrated an effectorless mutant strain of
121 *Pseudomonas syringae* DC3000, termed *P. syringae* DC3000(D36E), which did not
122 elicit observable defense responses or hydrogen peroxide accumulation in any maize
123 inbred line. These data thus suggest *P. syringae* induces defense responses in diverse
124 maize inbreds and that maize likely encodes disease resistance proteins that recognize
125 the activities of one or more *Pseudomonas* effectors.
126
127
128 **MATERIALS AND METHODS**
129 **Plant growth conditions**
130 Seed of maize inbreds were ordered from the North Central Regional Plant
131 Introduction Station via the National Plant Germplasm System Web Portal. Maize
132 inbreds were grown in plastic pots containing Berger Seed Germination and
133 Propagation Mix supplemented with Osmocote slow-release fertilizer (14-14-14). Plants
134 were maintained in a growth chamber with 16h:8h photoperiod, light:dark at 24°C with
135 light and 22°C in the dark and 60% humidity with average light intensities at plant height
136 of 130µmols/m^2/s.
137
138

139 ***Pseudomonas* growth conditions and leaf infiltration assay**

140 *Pseudomonas syringae* pv. *tomato* DC3000 and *Pseudomonas syringae*
141 DC3000(D36E) strains were grown on King's B (KB) medium supplemented with 25µg
142 of rifampicin and 50µg of kanamycin per milliliter for two days at 30°C. The
143 *Pseudomonas* strains were resuspended in 10mM $MgCl_2$ to an optical density at 600
144 nm (OD_{600}) of 0.5. Bacterial suspensions were infiltrated into the abaxial surface of the
145 second leaf of two-week old maize seedlings using a 1-mL disposable syringe, and the
146 infiltrated regions were indicated with a black permanent marker. The leaf surface was
147 nicked with a sterile razor blade prior to infiltration to facilitate fluid entry. The infiltrated
148 leaves were phenotyped five days following *Pseudomonas* infiltration and a
149 representative leaf was photographed under white light shortly thereafter.
150

151 **Histochemical detection of hydrogen peroxide accumulation**

152 Hydrogen peroxide (one of several reactive oxygen species) accumulation was
153 detected as previously described with slight modifications (Bach-Pages and Preston,
154 2017). Briefly, the *Pseudomonas* suspensions were infiltrated into two-week old maize
155 seedlings and, 3 days post-infiltration, leaf segments were harvested and incubated in
156 freshly prepared 3,3'-diaminobenzidine (DAB) solution (1 mg/mL (Sigma-Aldrich)
157 dissolved in distilled water (pH 3.8) overnight with gentle agitation in the dark. After
158 overnight incubation, the DAB-stained leaf tissues were rinsed with distilled water,
159 submerged in absolute ethanol, and incubated at 65℃ for 2 hours to clear the
160 chlorophyll. The leaf segments were rehydrated with 75% ethanol and incubated for 1
161 hour at room temperature, followed by incubation with 50% ethanol until the leaves

162 were cleared of chlorophyll. The cleared leaf tissue was stored in ultrapure water
163 (supplemented with 20% glycerol) for photography. Representative DAB-stained leaf
164 segments were photographed under white light.
165
166 **RNA extraction and reverse transcriptional real-time quantitative PCR of maize**
167 **defense genes**
168 Two-week old maize leaves (cvs. B73 [non-responder] and Mo18W [responder])
169 were infiltrated with *P. syringae* pv. *tomato* DC3000. The infiltrated leaf tissue was
170 harvested 12- and 24-hours post-*Pseudomonas* infiltration, flash frozen in liquid
171 nitrogen, and stored at -80C until processing. Total RNA was isolated using TRIzol
172 reagent from maize tissues according to the manufacturer's instruction (Direct-zol™
173 RNA miniprep, ZymoResearch) followed by in-column DNase I treatment. RNA
174 concentration was measured using Nanodrop (Thermo Scientific). Two micrograms of
175 total RNA were used for first-strand cDNA synthesis using AMV reverse transcriptase
176 (New England Biolabs). A quantitative real-time PCR (RT-qPCR) assay was performed
177 on a LightCycler 480 II system using 2x SYBR Green qPCR master mix (BioRad).
178 Maize GAPDH (Zm00001eb233140) was chosen as an endogenous reference gene to
179 normalize the data. Three technical replicates of the RT-qPCR assay were used for
180 each sample with a minimum of three biological replicates. Each biological replicate was
181 sampled from three individual plants. The transcript expression level was calculated
182 using the $2^{-\Delta\Delta CT}$ method (Livak and Schmittgen, 2001). The experiment was repeated at
183 least two independent times. Primers used for RT-qPCR are as follows (5' to 3'):
184 ZmGAPDH-FW (CCTGCTTCTCATGGATGGTT); ZmGAPDH-RV

185 (TGGTAGCAGGAAGGGAAACA); ZmPR3-FW (AGCTTCCTCGTCTCATCATCG);
186 ZmPR3-RV (TGTTGACGTAGGCGTAGAGC); ZmPR5-FW
187 (GCAGCCAGGACTTCTACGAC); ZmPR5-RV (CACAGGCATGGGTCTTCAC); ZmPAL-
188 FW (TCTGGTCCCGCTCTCCTACA); ZmPAL-RV (TTGAAGAAGCCGCCCTCGAT);
189 Peroxidase-FW (CTCATCAACCACCCGGACAC); Peroxidase-RV
190 (TGCAGCAAGCCTTATTTGAACA).
191
192
193 **RESULTS**
194 The observation that *P. syringae* pv. *tomato* DC3000 elicits robust immune
195 responses in crop plant species such as wheat led us to hypothesize that this bacterial
196 phytopathogen may also activate defense responses in maize inbreds. To test our
197 hypothesis, we infiltrated the parental inbred lines of the maize nested association
198 mapping population with *P. syringae* pv. *tomato* DC3000 and phenotyped their
199 responses five days post-*Pseudomonas* infiltration (Figure 1A). As a control, we
200 infiltrated *P. syringae* pv. *tomato* DC3000 into wheat leaves, which was previously
201 shown to recognize this bacterial pathogen (Ramachandran et al., 2017). In our
202 evaluations, we observed a variety of responses to *P. syringae* pv. *tomato* DC3000 and
203 scored the phenotypes as either no observable response (N) or as one of three
204 responses: weak chlorosis (WC), chlorosis (C) with minimal cell death, and
205 hypersensitive reaction (HR)-like cell death. Representative examples of phenotypic
206 responses are shown in Figure 1B, and a complete list of inbred lines and their
207 responses are shown in Table 1. Of the twenty-six maize inbreds tested, 13 were

208 scored as N, 2 as WC, and 2 as C (Figure 1B; Table 1). Nine maize inbred lines
209 (CML52, CML69, CML247, CML333, HP301, M162W, Mo18W, Ms71, and IL14H)
210 displayed a HR-like response to *P. syringae* pv. *tomato* DC3000 within the infiltrated
211 region (Figure 1B; Table 1). As a control, we infiltrated a mutant strain of *P. syringae* pv.
212 *tomato* DC3000, termed *P. syringae* DC3000(D36E), which lacks all endogenous
213 bacterial effectors (Wei et al., 2015; Carter et al., 2019). As expected, there was no
214 observable response in any inbred line tested to *P. syringae* DC3000(D36E) (Figure
215 1B). These data thus demonstrate the phenotypic responses observed in response to *P.*
216 *syringae* pv. *tomato* DC3000 are likely dependent upon recognition of one or more *P.*
217 *syringae* effectors.

218 The production and accumulation of reaction oxygen species, including hydrogen
219 peroxide, is often used as a proxy for activation of defense responses (Carter et al.,
220 2019). Therefore, we used 3,3'-diaminobenzidine (DAB) staining following leaf
221 infiltration with either *P. syringae* pv. *tomato* DC3000 or *P. syringae* DC3000(D36E) to
222 test whether the phenotypic responses of some maize inbred lines to *P. syringae* pv.
223 *tomato* DC3000 is correlated with hydrogen peroxide accumulation. Consistent with the
224 phenotypic responses, maize inbreds that displayed an HR-like cell death response to
225 *P. syringae* pv. *tomato* DC3000 accumulated detectable hydrogen peroxide within the
226 infiltrated region (Figure 2). In contrast, there was no hydrogen peroxide detected in
227 maize lines that did not recognize *P. syringae* pv. *tomato* DC3000 or in lines infiltrated
228 with *P. syringae* DC3000(D36E) (Figure 2). These results thus reveal the chlorotic and
229 HR-like cell death response in maize inbreds that recognize *P. syringae* pv. *tomato*
230 DC3000 is strongly correlated with the production and accumulation of ROS.

231 Though chlorotic and cell death responses are considered defense responses in
232 grasses (Smith and Mansfield, 1981; Yin and Hulbert, 2010; Carter et al., 2019), it was
233 unclear whether the *P. syringae* pv. *tomato* DC3000-mediated defense responses in
234 maize were correlated with increased defense gene expression. We, therefore, used
235 reverse transcription-quantitative polymerase chain reaction (RT-qPCR) to measure
236 mRNA abundance of a subset of defense-related maize genes in both non-responding
237 (B73) and a responding (Mo18W) maize inbred lines at 12- and 24-hours post-
238 *Pseudomonas* infiltration. In our analysis, we selected a subset of defense-related
239 maize genes whose transcriptional activation is associated with salicylic acid signaling
240 and which have been previously shown to be up-regulated during maize-pathogen
241 interactions (Przybylska et al., 2018; Shumilaket al., 2023). Consistent with the
242 phenotypic responses to *P. syringae* pv. *tomato* DC3000, transcript expression of the
243 selected defense genes was significantly upregulated in Mo18W when compared to B73
244 at 12- and 24-hours following *Pseudomonas* infiltration (Figure 3). Collectively, these
245 data clearly demonstrate *P. syringae* pv. *tomato* DC3000 activates robust defense
246 responses, including hydrogen peroxide accumulation as well as up-regulation of
247 defense-related genes, in diverse maize inbreds.
248
249
250 **DISCUSSION**
251 Our work presented here is, to the best of our knowledge, the first to show that *P.*
252 *syringae* pv. *tomato* DC3000 elicits HR-like cell death in some maize inbreds.
253 Consistent with our observations, this bacterial pathogen also induces defense

254 responses in both *Nicotiana benthamiana* and soybean via the recognition of the
255 HopQ1-1 and AvrD effectors, respectively (Kobayashi et al., 1989; Wei et al., 2007).
256 Though our work shows that maize recognizes *P. syringae* pv. *tomato* DC3000, it
257 remains unknown which *Pseudomonas* effectors are specifically recognized. To this
258 end, Ruiz-Bedoya and colleagues (2023) recently generated thirty-six coisogenic
259 *Pseudomonas* strains, each expressing a single *Pseudomonas* effector in the
260 effectorless *P. syringae* DC3000(D36E) mutant. Hence, future research efforts will focus
261 on infiltrating the library of *P. syringae* DC3000(D36E) coisogenic strains in maize to
262 determine which bacterial effectors are specifically recognized (Ruiz-Bedoya et al.,
263 2023). Such knowledge will be valuable in determining the molecular and cellular
264 mechanisms underlying nucleotide-binding leucine-rich repeat immune receptors (NLR)-
265 dependent recognition of *P. syringae* pv. *tomato* DC3000 effectors (Prigozhin et al.,
266 2022; Thatcher et al., 2023).

267 The observation that *P. syringae* pv. *tomato* DC3000 elicits defense responses in
268 maize suggests this bacterial pathogen can be utilized as a surrogate for expression of
269 crop pathogen effectors in maize. Indeed, the bacterial type III secretion system from *P.*
270 *syringae* pv. *tomato* DC3000 has been effectively used to deliver candidate effector
271 proteins directly inside host cells to ascertain effector functions (Fabro et al., 2011; Qi et
272 al., 2018; Ramachandran et al., 2017; Sohn et al., 2007). Development of a *P. syringae*
273 pv. *tomato* DC3000-based heterologous expression system in maize will thus likely
274 facilitate the functional screening of effector proteins from obligate biotrophic pathogens
275 of maize. For example, effector proteins from the maize fungal pathogens *Ustilago*
276 *maydis* and *Puccinia polyspora* suppress PAMP-elicited reactive oxygen species

277 production (Chen et al., 2022; Navarrete et al., 2021; Saado et al., 2022). However, it
278 remains unknown whether these crop pathogen effectors are capable of suppressing *P.*
279 *syringae* pv. *tomato* DC3000-mediated defense responses in maize.

280 In summary, we show that *P. syringae* pv. *tomato* DC3000, but not the
281 effectorless mutant, induces robust defense responses in some maize inbreds. Though
282 it is unclear which *P. syringae* pv. *tomato* DC3000 effectors are recognized, our data
283 nevertheless suggests maize likely encodes disease resistance proteins that recognize
284 the activities of one or more *Pseudomonas* effectors. Future research efforts will, in
285 part, focus on fine mapping the genetic loci responsible for *P. syringae* pv. *tomato*
286 DC3000 recognition.

287

288

289 **ACKNOWLEDGEMENTS**

290 We thank the North Central Regional Plant Introduction Station for providing
291 seed of the maize inbred lines and Dr. Terri Cameron (USDA-ARS) for their technical
292 assistance and maintenance of maize germplasm.

293

294

295

296

297

298

299

300 **LITERATURE CITED**

301 **Abramovitch, R.B., Kim, Y.J., Chen, S., Dickman, M.B., and Martin, G.B.** 2003.
302 *Pseudomonas* type III effector AvrPtoB induces plant disease susceptibility by
303 inhibition of host programmed cell death. EMBO J. 22: 60–69.

304 **Bach-Pages, M., and Preston, G.** 2017. Methods to quantify biotic-induced stress in
305 plants. Methods Mol Biol. 1734: 241-255.

306 **Benson, J., Poland, J., Benson, B., Stromberg, E., and Nelson, R.** 2015. Resistance
307 to Gray Leaf Spot of Maize: Genetic Archtecture and Mechansisms Elucidated
308 through Nested Association Mapping and Near-Isogenic Line Analysis. PLoS
309 Genet 11: e1005045.

310 **Bentham, A., De la Concepcion, J., Mukhi, N., Zdrzalek, R., Draeger, M., Gorenkin,**
311 **D., Hughes, R., and Banfield, M.** 2020. A molecular roadmap to the plant
312 immune system. J Biol Chem. 295: 14916-14935.

313 **Boller, T., and Felix, G.** 2009. A renaissance of elicitors: perception of microbe
314 associated molecular patterns and danger signals by pattern-recognition
315 receptors. Annu. Rev. Plant Biol. 60: 379–406.

316 **Carter, M.E., Helm, M., Chapman, A.V.E., Wan, E., Restrepo-Sierra, A.M., Innes,**
317 **R.W., Bogdanove, A.J., and Wise, R.P.** 2019. Convergent evolution of effector
318 protease recognition by *Arabidopsis* and barley. Mol Plant-Microbe Interact. 32:
319 550-565.

320 **Chakravarthy, S., Worley, J.N., Rodriguez-Montes, A., and Collmer, A.** 2018.
321 *Pseudomonas syringae* pv. *tomato* DC3000 polymutants deploying coronatine
322 and two type III effectors produce quantifiable chlorotic spots from individual

323 bacterial colonies in *Nicotiana benthamiana* leaves. Mol Plant Pathol 19: 935-
324 947.
325 **Chen, G., Zhang, B., Ding, J., Wang, H., Deng, C., Wang, J., Yang, Q., Pi, Q.,**
326 **Zhang, R., Zhai, H., Dong, J., Huang, J., Hou, J., Wu, J., Que, J., Zhang, F.,**
327 **Li, W., Min, H., Tabor, G., Li, B., Liu, X., Zhao, J., Yan, J., and Lai, Z**. 2022.
328 Cloning southern rust resistant gene RppK and its cognate gene AvrRppK from
329 Puccinia polyspora. Nat. Commun. 13, 4392.
330 **Chen, J., Zhang, X., Rathjen, J.P., and Dodds, P.N.** 2022. Direct recognition of
331 pathogen effectors by plant NLR immune receptors and downstream signaling.
332 Essays Biochem 66: 471-483.
333 **Coll, N.S., Epple, P., and Dangl, J.L.** 2011. Programmed cell death in the plant
334 immune system. Cell Death Differ. 18: 1247-1256.
335 **Fabro, G., Steinbrenner, J., Coates, M., Ishaque, N., Baxter, L., Studholme, D.J.,**
336 **Körner, E., Allen, R.L., Piquerez, S.J.M., Rougon-Cardoso, A., Greenshields,**
337 **D., Lei, R., Badel, J.L., Caillaud, M.-C., Sohn, K.-H., Van den Ackerveken, G.,**
338 **Parker, J.E., Beynon, J., and Jones, J.D.G**. 2011. Multiple candidate effectors
339 from the oomycete pathogen *Hyaloperonospora Arabidopsis* suppress host plant
340 immunity. PLOS Pathog 7: e1002348.
341 **Ferrante, P., Clarke, C.R., Cavanaugh, K.A., Michelmore, R.W., Buonaurio, R., and**
342 **Vinatzer, B.A.** 2009. Contributions of the effector gene hopQ1-1 to differences in
343 host range between *Pseudomonas syringae pv. phaseolicola* and *P. syringae pv.*
344 *tabaci*. Mol Plant Pathol 10: 837–842.
345

346 **Gage, J.L., Monier, B., Giri, A., and Buckler, E.S.** 2020. Ten Years of the Maize
347 Nested Association Mapping Population: Impact, Limitations, and Future
348 Directions. Plant Cell. 32: 2083–2093.
349 **Giska, F., Lichocka, M., Piechocki, M., Dadlez, M., Schmelzer, E., Hennig, J., and**
350 **Krzymowska, M.** 2013. Phosphorylation of HopQ1, a Type III Effector from
351 *Pseudomonas syringae*, creates a binding site for host 14-3-3 proteins. Plant
352 Physiol 161: 2049–2061.
353 **Guo, M., Tian, F., Wamboldt, Y., and Alfano, J.R.** 2009. The majority of the type III
354 effector inventory of *Pseudomonas syringae pv. tomato* DC3000 can suppress
355 plant immunity. Mol. Plant–Microbe Interact. 22: 1069–1080.
356 **Jamir, Y., Guo, M., Oh, H.-S., Petnicki-Ocwieja, T., Chen, S., Tang, X., Dickman,**
357 **M.B., Collmer, A., and Alfano, J.R.** 2004. Identification of *Pseudomonas*
358 *syringae* type III effectors that can suppress programmed cell death in plants and
359 yeast. Plant J. 37: 554–565.
360 **Kobayashi, D., Tamaki, S., and Keen, N.** 1989. Cloned avirulence genes from the
361 tomato pathogen Pseudomonas syringae pv. tomato confer cultivar specificity on
362 soybean. Proc Natl Acad USA 86: 157-161.
363 **Kump, K., Bradbury, P., Wisser, R., Buckler, E., Belcher, A., Oropeza-Rosas, M.,**
364 **Zwonitzer, J., Kresovich, S., McMullen, M., Ware, D., Balint-Kurti, P., and**
365 **Holland, J.** 2011. Genome-wide association study of quantitative resistance to
366 southern leaf blight in the maize nested association mapping population. Nat
367 Genet. 43: 163-168.
368

369 **Kvitko, B.H., Park, D.H., Velasquez, A.C., Wei, C.-F., Russell, A.B., Martin, G.B.,**
370 **Schneider, D.J. and Collmer, A.** 2009. Deletions in the repertoire of
371 *Pseudomonas syringae pv. tomato* DC3000 type III secretion effector genes
372 reveal functional overlap among effectors. PLoS Pathog. 5: e1000388.
373 **Li, G., Froehlich, J., Elowsky, C., Msanne, J., Ostosh, A., Zhang, C., Awada, T., and**
374 **Alfano, J.** 2014. Distinct Pseudomonas type-III effectors use a cleavable transit
375 peptide to target chloroplast. Plant J 77:310-321.
376 **Li, W., Yadeta, K.A., Elmore, J.M., and Coaker, G.** 2013. The *Pseudomonas* effector
377 HopQ1 promotes bacterial virulence and interacts with tomato 14-3-3 proteins in
378 a phosphorylation dependent manner. Plant Physiol 161: 2062–2074.
379 **Livak, K.J., and Schmittgen, T.D.** 2001. Analysis of relative gene expression data
380 using real-time quantitative PCR and the 2(-delta delta C(T)) method. Methods
381 25: 402-408.
382 **Lovelace, A., Dorhmi, S., Hulin, M., Li, Y., Mansfield, J., and Ma, W.** 2023. Effector
383 identification in plant pathogens. Phytopathology 113: 637-650.
384 **Lozano-Duran, R., Bourdais, G., He, S.Y., and Robatzek, S.** 2014. The bacterial
385 effector HopM1 suppresses PAMP-triggered oxidative burst and stomatal
386 immunity. New Phytol. 202: 259–269.
387 **Martin, G.B.** 2012. Suppression and activation of the plant immune system by
388 *Pseudomonas syringae* effectors AvrPto and AvrPtoB. In: Effectors in Plant–
389 Microbe Interactions (eds F. Martin and S. Kamoun), 123–154 (Wiley-Blackwell,
390 2011).
391

392 **Navarrete, F., Grujic, N., Stirnberg, A., Saado, I., Aleksza, D., Gallei, M., Adi, H.,**
393 **Alcantara, A., Khan, M., Bindics, J., Trujillo, M., and Djamei, A.** 2021. The
394 Pleiades are a cluster of fungal effectors that inhibit host defenses. PLoS Pathog
395 17: e1009641
396 **Ngou, B.P.M., Ding, P., and Jones, J.D.G.** 2022. Thirty years of resistance: Zig-zag
397 through the plant immune system. Plant Cell 34:1447-1478.
398 **Poland, J., Bradbury, P., Buckler, E., and Nelson, R.** 2011. Genome-wide nested
399 association mapping of quantitative resistance to northern leaf blight in maize.
400 Proc Natl Acad Sci USA 108: 6893-6898.
401 **Prigozhin, D., Rangavajjhala, S., and Krasileva, K**. 2022. Majority of the highly
402 variable NLRs in maize share genomic location and contain additional target-
403 binding domains. bioRxiv DOI: https://doi.org/10.1101/2022.10.05.510735
404 **Przybylska, A., Kornobis, F., and Obrepalska-Steplowska, A.** 2018. Analysis of
405 defense gene expression changes in susceptible and tolerante cultivars of maize
406 (Zea mays) upon Meloidogyne arenaria infection. Physiol Mol Plant Pathol 103:
407 78-83.
408 **Qi, M., Grayczyk, J.P., Seitz, J.M., Lee, Y., Link, T.I., Choi, D., Pedley, K.F.,**
409 **Voegele, R.T., Baum, T.J., and Whitham, S.A**. 2018. Suppression or activation
410 of immune responses by predicted secreted proteins of the soybean rust
411 pathogen *Phakopsora pachyrhizi*. Mol Plant-Microbe Interact 31: 163-174.
412 **Ramachandran, S.R., Yin, C., Kud, J., Tanaka, K., Mahoney, A.K., Xiao, F., and**
413 **Hulbert, S.H.** 2017. Effectors from wheat rust fungi suppress multiple plant
414 defense responses. Phytopathology 107: 75-83.

415 **Ruiz-Bedoya, T., Wang, P., Desveaux, D., and Guttman, D.** 2023. Cooperative
416 virulence via the collective action of secreted pathogen effectors. Nat Microbiol 8:
417 640-650.
418 **Saado, I., Chia, K-S., Betz, R., Alcantara, A., Pettko-Szandtner, A., Navarrete, F.,**
419 **D'Auria, J., Kolomiets, M., Melzer, M., Feussner, I., and Djamei, A**. 2022.
420 Effector-mediated relocalization of a maize lipoxygenase protein triggers
421 susceptibility to Ustilago maydis. Plant Cell 34: 2785-2805.
422 **Shumilak, A., El-Shetehy, M., Soliman, A., Tambong, J., and Daayf, F**. 2023. Goss's
423 wilt resistance in corn is mediated via salicylic acid and programmed cell death
424 but not jasmonic acid pathways. Plants 12: 1475.
425 **Singh, R., Shim, S., Telenko, D.E.P., and Goodwin, S**. 2023. Parental inbred lines of
426 the Nested Association Mapping (NAM) population of corn show sources of
427 resistance to tar spot in Northern Indiana. Plant Dis. 107: 262-266.
428 **Smith, J.J., and Mansfield, J.W**. 1981. Interactions between pseudomonads and
429 leaves of oats, wheat and barley. Physiol. Plant Pathol. 18: 345-IN317.
430 **Sohn, K.H., Lei, R., Nemri, A., and Jones, J.D.G.** 2007. The downy mildew effector
431 proteins ATR1 and ATR13 promote disease susceptibility in *Arabidopsis thaliana*.
432 Plant Cell 19: 4077.
433 **Thatcher, S., Jung, M., Panangipalli, G., Fengler, K., Sanyal, A., Li, B., Llaca, V.,**
434 **and Habben, J.** 2023. The NLRomes of Zea mays NAM founder lines and Zea
435 luxurians display presence-absence variation, integrated domain diversity, and
436 mobility. Mol Plant Pathol 24: 742-757.
437

438 **Wei, C-F., Kvitko, B.H., Shimizu, R., Crabill, E., Alfano, J.R., Lin, N.-C., Martin,**
439 **G.B., Huang, H.-C., and Collmer, A.** 2007. A *Pseudomonas syringae pv. tomato*
440 DC3000 mutant lacking the type III effector HopQ1-1 is able to cause disease in
441 the model plant *Nicotiana benthamiana*. Plant J. 51: 32–46.
442 **Wei, H.-L., Chakravarthy, S., Mathieu, J., Helmann, T.C., Stodghill, P., Swingle, B.,**
443 **Martin, G.B. and Collmer, A**. 2015. *Pseudomonas syringae pv. tomato* DC3000
444 type III secretion effector polymutants reveal an interplay between HopAD1 and
445 AvrPtoB. Cell Host Microbe 17: 752–762.
446 **Wei, H-L., and Collmer, A.** 2018. Defining essential processes in plant pathogenesis
447 with *Pseudomonas syringae* pv. *tomato* DC3000 disarmed polymutants and a
448 subset of key type III effectors. Mol Plant Pathol 19: 1779-1794.
449 **Xin, X-F., and He, S.Y.** 2013. Pseudomonas syringae pv. tomato DC3000: a model
450 pathogen for probing disease susceptibility and hormone signaling in plants.
451 Annu Rev Phytopathol 51: 473-498.
452 **Yin, C., and Hulbert, S**. 2010. Prospects for functional analysis of effectors from cereal
453 rust fungi. Euphytica 179: 57-67.
454
455
456
457
458
459
460

461 **FIGURE LEGENDS**

462

463 **Figure 1. *Pseudomonas syringae* pv. *tomato* DC3000 induces defense responses**
464 **in maize. A)** Schematic diagram of the *Pseudomonas* HR assay. The *P. syringae* pv.
465 *tomato* DC3000 and *P. syringae* DC3000(D36E) strains were resuspended in 10mM
466 $MgCl_2$. The bacterial suspensions were adjusted to an optical density at 600nm (OD_{600})
467 of 0.5 and syringe-infiltrated into the underside surface of the second leaf (L2) of two-
468 week old maize seedlings. The infiltrated regions were marked with a black permanent
469 marker. **B)** Responses of the maize inbred lines to either *P. syringae* pv. *tomato*
470 DC3000 or *P. syringae* DC3000(D36E) were phenotyped five days following infiltration.
471 Responses were scored as N, no observable response; WC, weak chlorosis; C,
472 chlorosis with cell death; and HR, hypersensitive reaction. Wheat cv. Fielder inoculated
473 with either *P. syringae* pv. *tomato* DC3000 or *P. syringae* DC3000(D36E) was used as a
474 control (Carter et al., 2019; Ramachandran et al., 2017).

475

476 **Table 1. Responses of the twenty-six inbred maize lines of the nested association**
477 **mapping (NAM) to *Pseudomonas syringae* pv. *tomato* DC3000.** Accession numbers,
478 origins, and market class were mined from the Maize Genetics and Genomics
479 Database.

480

481 **Figure 2: Maize lines accumulated detectable hydrogen peroxide in response to**
482 ***P. syringae* pv. *tomato* DC3000.** Representative maize inbreds assayed and
483 *Pseudomonas* treatments were as in Figure 1B. Three days following *Pseudomonas*

484 infiltration, leaf segments were harvested from the infiltrated regions and stained
485 overnight with 3,3'-diaminobenzidine (DAB) solution. After overnight incubation, the leaf
486 tissue was rinsed with deionized water, cleared with ethanol to remove the chlorophyll,
487 and stored in ultrapure water (supplemented with 20% glycerol) for photography. Wheat
488 cv. Fielder inoculated with either *P. syringae* pv. *tomato* DC3000 or *P. syringae*
489 DC3000(D36E) was used as a control.
490
491 **Figure 3: *P. syringae* pv. *tomato* DC3000 significantly increases transcript**
492 **expression of maize defense genes.** Reverse transcription-quantitative polymerase
493 chain reaction (RT-qPCR) expression analyses of selected maize defense genes:
494 Pathogenesis-related 3 (ZmPR3), Pathogenesis-related 5 (ZmPR5), Phenylalanine
495 Ammonia Lyase (ZmPAL), and peroxidase in response to *P. syringae* pv. *tomato*
496 DC3000. Two-week old maize leaves (cvs. B73 [non-responder] and Mo18W
497 [responder]) were infiltrated with *P. syringae* pv. *tomato* DC3000. The infiltrated leaf
498 tissue was harvested 12- and 24-hours post-*Pseudomonas* infiltration, flash frozen in
499 liquid nitrogen, and stored at -80°C until processing. Total RNA extraction followed by
500 cDNA preparation and expression of defense genes was quantified by RT-qPCR.
501 Values represent mean ± S.D. (n = 3) from three biological replicates and three technical
502 replicates in each experiment. The maize GAPDH gene was used as an internal
503 reference gene. The gene expression in B73 plants at 12 hours after *P. syringae* pv.
504 *tomato* DC3000 infiltration was set to 1. Multiple comparisons were conducted by two-
505 way ANOVA followed by the Šídák's method. One asterisk (*) indicates $P<0.05$, two (**)
506 $P<0.01$, three (***) $P<0.001$, and four (****) $P<0.0001$.

507 **Figure 1**

A

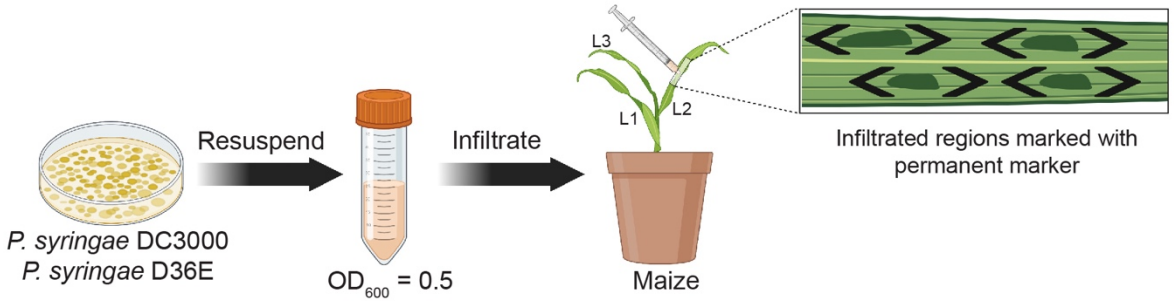

B

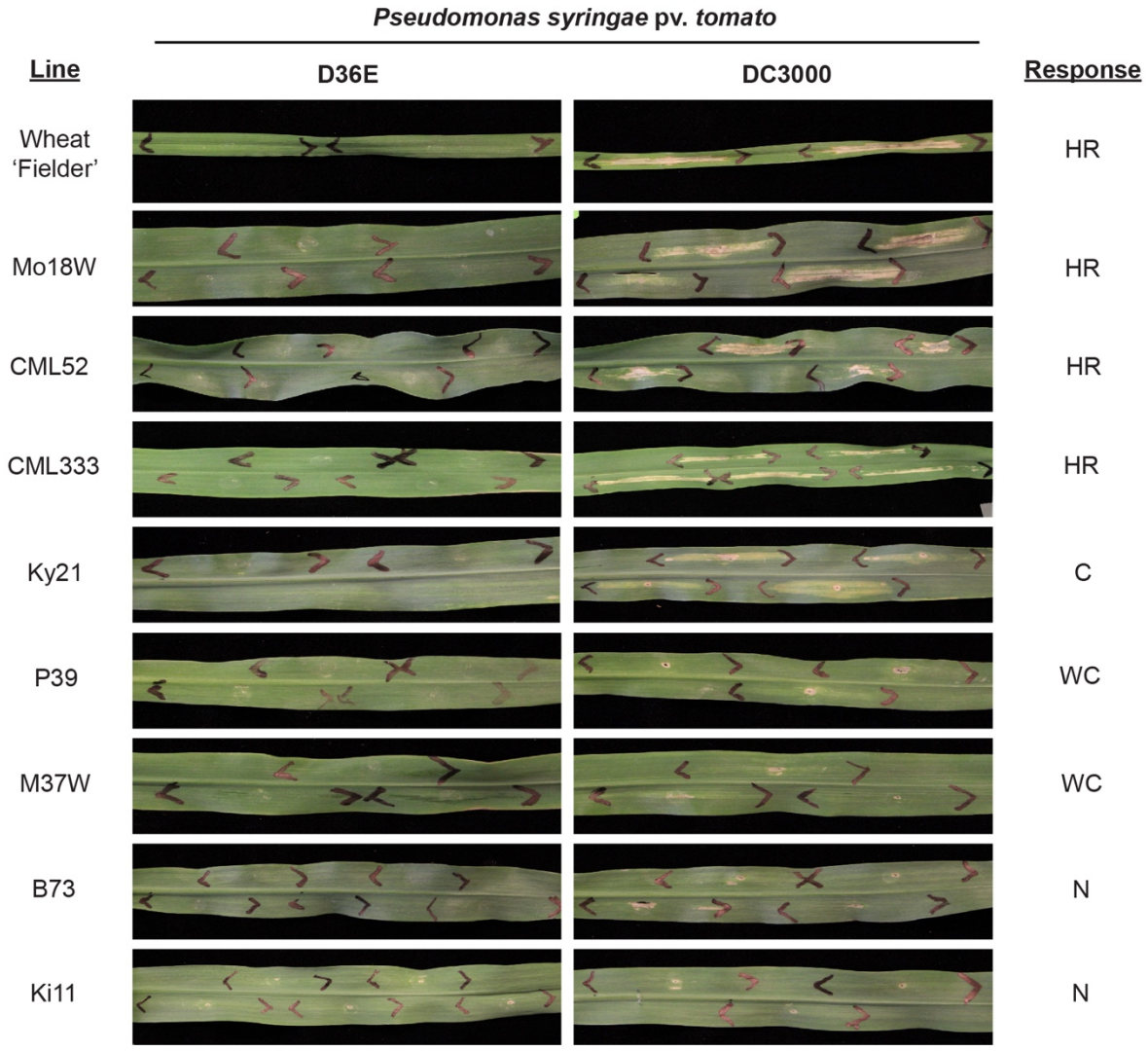

508

509

510

511 **Table 1**

Line[a]	Accession	Origin	Market Class	Response[b]
CML52	PI 595561	Ciudad de Mexico, Mexico	Yellow flint	HR
CML69	PI 690318	Ciudad de Mexico, Mexico	Yellow dent	HR
CML247	PI 595541	Ciudad de Mexico, Mexico	White dent	HR
CML333	PI 690322	Ciudad de Mexico, Mexico	White flint	HR
HP301	PI 587131	Indiana, United States	Popcorn	HR
M162W	PI 690328	KwaZulu-Natal, South Africa		HR
Mo18W	PI 550441	Missouri, United States	White dent	HR
Ms71	PI 587137	Michigan, United States		HR
IL14H	PI 690323	Illinois, United States	Sweetcorn	HR
CML277	PI 595550	Ciudad de Mexico, Mexico	White flint	C
Ky21	PI 690326	Kentucky, United States	White dent	C
P39	PI 587133	Indiana, United States	Sweetcorn	WC
M37W	PI 690327	KwaZulu-Natal, South Africa		WC
B73	PI 550473	Iowa, United States	Yellow dent	N
B97	PI 564682	Iowa, United States	Yellow dent	N
CML103	PI 690319	Ciudad de Mexico, Mexico	White dent	N
CML228	PI 690320	Ciudad de Mexico, Mexico	Yellow flint	N
CML322	PI 690321	Ciudad de Mexico, Mexico	White flint	N
Ki3	PI 690324	Thailand	Yellow flint	N
Ki11	PI 690325	Thailand		N
NC350	PI 690329	North Carolina, United States		N
Oh7B	PI 690331	Ohio, United States		N
Oh43	PI 690332	Ohio, United States	Yellow dent	N
Tx303	PI 690334	Texas, United States	Yellow dent	N
Tzi8	PI 506246	Oyo, Nigeria	White flint	N
NC358	PI 690330	North Carolina, United States		N

a Parental inbred lines from the maize Nested Association Mapping (NAM) population.

b Maize leaves (L2) of 14-day-old plants were infiltrated, using a needleless syringe, with a *P. syringae pv. tomato* DC3000 suspension at an optical density at 600 nm (OD_{600}) of 0.5 and photographed 5 days post-infiltration (5dpi). Phenotypes were scored as: N, no ressponse; WC, weak chlorosis; C, chlorosis; and HR, hypersensitive reaction.

512

513

514

515

516

517

518

519

520

521

522

523 **Figure 2**

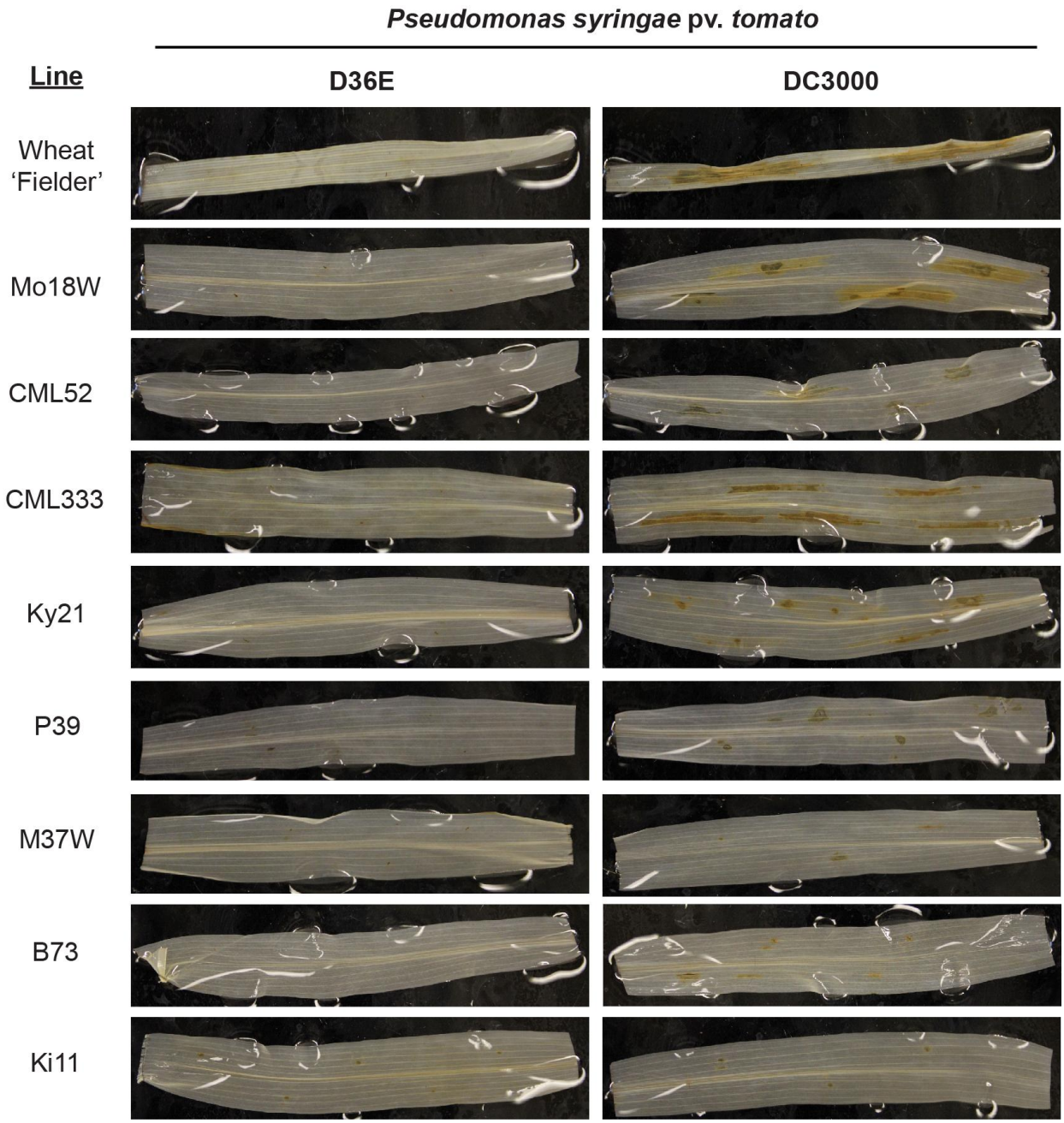

524

525

526

527

528

Figure 3

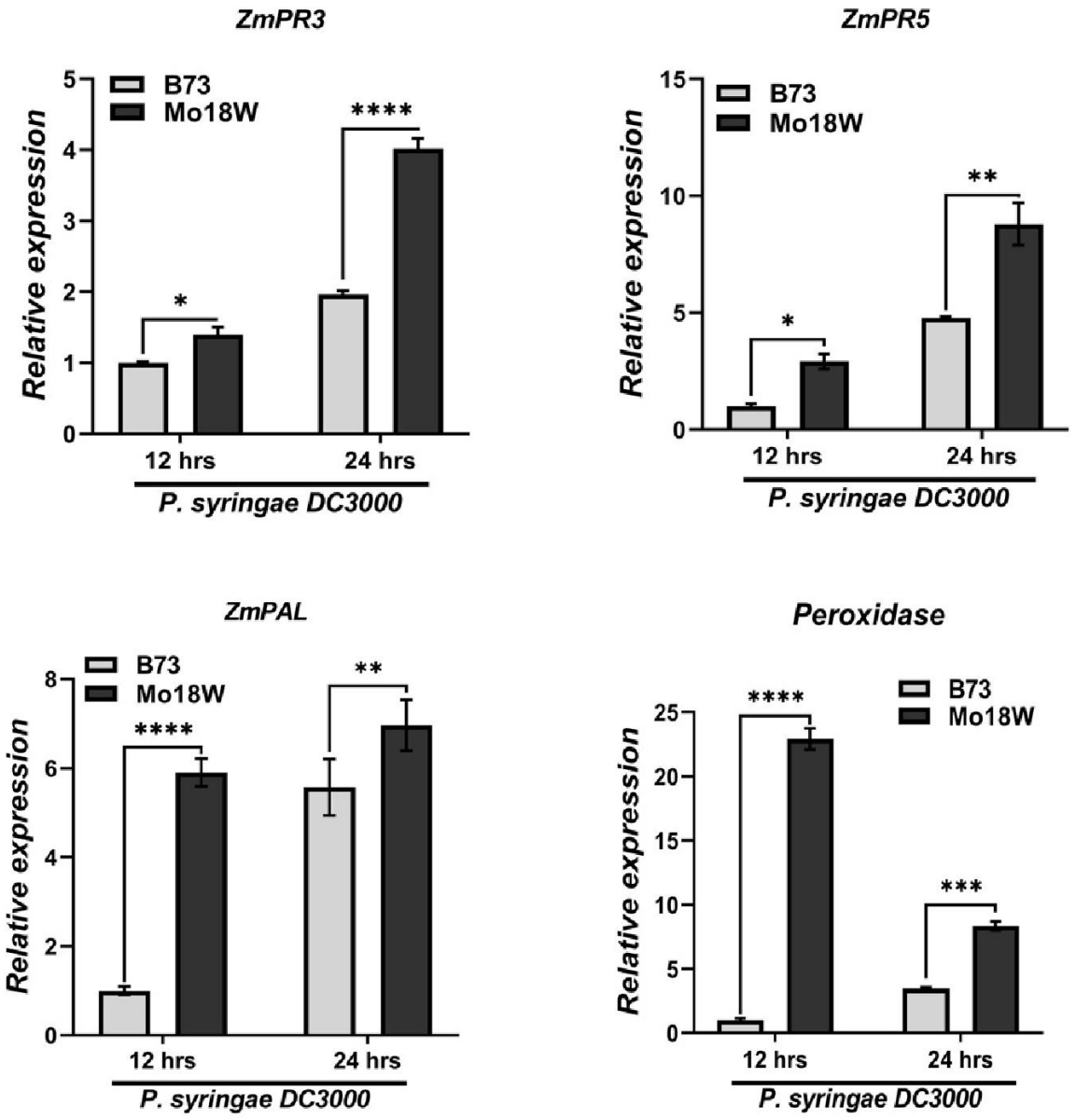
ZmPR3
B73
Mo18W
Relative expression
0
1
2
3
4
5
*
****
12 hrs
24 hrs
P. syringae DC3000
ZmPR5
B73
Mo18W
Relative expression
0
5
10
15
*
**
12 hrs
24 hrs
P. syringae DC3000
ZmPAL
B73
Mo18W
Relative expression
0
2
4
6
8
****
**
12 hrs
24 hrs
P. syringae DC3000
Peroxidase
B73
Mo18W
Relative expression
0
5
10
15
20
25
****
***
12 hrs
24 hrs
P. syringae DC3000